



## Design and Development of Rifampicin Nano-Bio-composite for the application of Anti-Microbial activity

Monali M Dumore<sup>1</sup>, Sharmila S Shah<sup>2</sup>, Nitin G Dumore<sup>3</sup>, Kuldeep H Ramteke<sup>4</sup>, Dhiraj Nikam<sup>5</sup>.

1305

1. Dadasaheb Balpande College of Pharmacy, Besa, Nagpur, MH, India
2. SVPMS College of Pharmacy, Malegaon Bk., Baramati, MH, India
3. Dadasaheb Balpande college of Diploma in Pharmacy, Besa, Nagpur, MH, India
4. Shivajirao Pawar College of Pharmacy, Ahmednagar, MH, India.
5. Bharati Vidyapeeth College of Pharmacy, Navi Mumbai, MH, India.

### Abstract:

In order to increase the antimicrobial activity of silver nanoparticles (AgNPs) against both Gram-positive (*Staphylococcus aureus*) and Gram-negative (*Escherichia coli*) bacteria, rifampicin antibiotic was loaded onto the AgNPs. In order to create AgNPs with a consistent prism shape, sodium borohydride (NaBH<sub>4</sub>), lactose, and sodium citrate were used in the preparation process. Finally, rifampicin was added to the produced AgNPs to functionalize them and create an AgNPs-rifampicin composite. The produced nanocomposites were characterised using a variety of analytical methods, including transmission electron microscopy (TEM) and ultraviolet-visible (UV-Vis) absorption spectra. According to the preparation procedures, AgNPs' average particle size and distribution varied slightly as seen in TEM pictures. AgNPs-rifampicin composites' antimicrobial activity was examined using the disc diffusion method. The prism AgNPs-rifampicin showed a considerable enhancement in antimicrobial activity against both kinds of bacteria, according to the results. Because of the vertexes and edges of nano prisms, which facilitate Ag ions' entry into the cell wall. Due to the different compositions of Gram-positive and Gram-negative bacteria's cell walls, AgNPs-rifampicin composites showed greater antibacterial efficacy against the former than the latter.

**Keywords:** Antimicrobial activity, Rifampicin, Silver nanoparticles, Nanobiocomposite, etc.

**DOI Number:** 10.14704/nq.2022.20.11.NQ66121

**NeuroQuantology 2022; 20(11): 1305-1315**

### Introduction

There are numerous uses for nanotechnology in electronics, cosmetics, energy, catalysis, and pharmaceuticals. The nanomaterial's extensive surface area is related to the wide range of optical, chemical, and mechanical capabilities that it possesses. The ability to regulate surface energy, surface area, and add specificity to the synthesised material's mechanism of action by adjusting particle size at the nanoscale is well established. Due to their small size and high surface energy, nanoparticles must be stabilised with an appropriate capping agent. Nanoparticle medications have been proven successful in treating deadly conditions like cancer,

hepatitis, and diabetes. Nanomedicines offer many benefits, including improved tissue absorption, selectivity in their mode of action, and improved intracellular tissues. Some treatments based on nanotechnology that treat terrible diseases are currently undergoing clinical testing, and others are already on the market<sup>[1-7]</sup>.

One of the main causes of the formation of multidrug-resistant pathogenic bacteria is the needless and indiscriminate use of antibiotics. Additionally, there is growing concern over biofilm-associated infections that are resistant to the current antibiotic arsenal, leaving little room for treatment. Therefore, it is essential



to discover alternative antibacterial agents. Recently, it has been discovered that microbes are killed either by microbicidal effects of the metal nanoparticles, such as release of free metal ions leading to cell membrane damage, DNA interactions, or free radical generation (Fenton reaction), or by micro biostatic effects combined with killing that are amplified by the host's immune system [8,9].

Chronic infections and death are frequently brought on by bacterial infections. Because of their low cost and efficient results, antibiotics have been the go-to treatment for bacterial illnesses. However, a number of studies have offered concrete proof that the extensive use of antibiotics has contributed to the creation of bacterial strains that are multidrug resistant. Antibiotic overuse has really recently led to the development of super-bacteria that are resistant to almost all antibiotics. These bacteria exhibit the super-resistance gene NDM-1, according to studies. Three bacterial targets are the focus of the main classes of antibiotics currently in use: the machinery involved in DNA replication, translation, and cell wall construction. Unfortunately, each of these mechanisms of action is susceptible to bacterial resistance [10,11].

Materials that have at least one dimension (1–100 nm) in the nanometer scale range or whose fundamental unit in three-dimensional space is in this range are referred to as nanomaterials. Particularly NPs have proven to provide broad-spectrum antibacterial effects against both Gram-positive and Gram-negative microorganisms. For instance, Ag NPs show concentration-dependent antibacterial action against *Escherichia coli* and *Pseudomonas aeruginosa*, and ZnO NPs were discovered to inhibit *Staphylococcus aureus*. The specific antibacterial actions of NPs, however, have not been fully elucidated, and the same NP types frequently exhibit divergent effects. According to one of three

models—oxidative stress induction, metal ion release, or non-oxidative mechanisms—NPs' antibacterial mechanism of action is typically explained. These three different mechanisms can all take place at the same time. According to certain research, Ag NPs cause the bacterial membrane's surface electric charge to be neutralised and alter its penetrability, which ultimately results in bacterial death [12-14].

A semi-synthetic, broad-spectrum antibiotic known as rifampicin is frequently used to treat tuberculosis [15,16]. But this medication also works to treat *Staphylococcus aureus* infections that are resistant to methicillin [17]. With its ability to penetrate deep tissues or living cells as well as its RNA polymerase inhibitory activity, it significantly reduced the length of time needed for TB chemotherapy as well as other chronic, life-threatening bacterial infections after its discovery. It is said to be able to cure a variety of biofilm-related illnesses because of its penetrating capacity [18,19]. Researchers have discovered many strategies to increase its bioavailability while minimising negative effects with the passage of time, the emergence of microbial resistance, and taking these factors into consideration [20]. By shrinking current antibiotics to the nanoscale, which increases cell permeability, nanotechnology gives them additional value. Recently, gentamicin and chlorhexidine nanoconjugate demonstrated improved biofilm inhibition and eradication efficiency [21,22]. The antibiotic rifampicin has excellent antibacterial activity and is particularly effective against Gram-positive and Gram-negative bacteria. Since this antibiotic is liposoluble, penetration into the majority of tissues is adequate. Rifampin is an antibiotic that prevents sensitive cells from producing DNA-dependent RNA polymerase. [25]

In this study, two composites of AgNPs and the antibiotic rifampin were created, described, and tested for their ability to fight both Gram-positive and Gram-negative



bacterial strains. Different capping materials, including sodium-borohydride, lactose, and a modified citrate approach, were used to create the AgNPs in a variety of shapes and sizes before being loaded with the antibiotic rifampin. <sup>(26)</sup> Using UV-VIS absorption spectra and TEM to explore their spectral, morphological nature, and chemical composition, the produced AgNPs and rifampin silver nanoparticle composites were assessed for their physicochemical properties. <sup>(25)</sup> To compare the antimicrobial activity of the generated AgNPs, Rifampin silver nanoparticles composite, and pure rifampin, their antimicrobial activity was evaluated using the Modified Kirby-Bauer disc diffusion method. As far as we are aware, this is the first study to look at the antibacterial activity of a nanocomposite made of rifampin silver nanoparticles against both gram-positive and gram-negative bacteria. <sup>(27)</sup>

## Materials and methods

### Materials

Tri-sodium citrate dehydrate, Lactose, Silver nitrate AgNO<sub>3</sub>, Sodium borohydride NaBH<sub>4</sub>, and Polyvinylpyrrolidone PVP were all bought from Sigma-Aldrich. We received a free sample of rifampicin from Banson Pharmaceuticals.

### Preparation of silver nanoparticles

AgNPs' distinct characteristics are influenced by their techniques of manufacture, forms, and sizes, all of which have a significant impact on their antibacterial activity. The two techniques of preparation were a green synthesis method utilising lactose to produce AgNPs in spherical and prism shapes with various diameters, and a chemical reduction method using tri-sodium citrate and NaBH<sub>4</sub>.

### Sodium borohydride assisted synthesis of silver nanoparticles [AgNPs (Borohydride)]

According to Multifinger and colleagues' procedure, 30 ml of ice-cold 2 mM NaBH<sub>4</sub> solution was stirred vigorously while 10 ml of 1 mM AgNO<sub>3</sub> was added drop-by-drop. Before use, the resulting colloidal solution was incubated for 24 hours and agitated for 1 hour. With the help of TEM and UV-VIS absorption spectroscopy, the morphology and optical characteristics of the produced particles were identified.

### Lactose assisted synthesis of silver nanoparticles [AgNPs (Lactose)]

A 250 ml 3-Necked flask was filled with 100 ml of 1 mM AgNO<sub>3</sub> and the recommended amount of lactose, according to the Madrakian et al. method (Madrakian et al., 2015). (5 g). At 80°C, the reaction vessel was vigorously stirred. Both TEM and UV-VIS absorption spectroscopy were used to study the morphology and optical characteristics of the produced particles.

### Citrate assisted synthesis of silver nanoparticle [AgNPs (Citrate)]

The chemical reduction of AgNO<sub>3</sub> was used to create spherical AgNPs in an aqueous media with little alterations. Metho Guzmán claims this. In this procedure, sodium citrate served as a stabiliser for the generated particles while NaBH<sub>4</sub> reduced Ag<sup>+1</sup> ion. PVP also served as another capping agent for any more AgNPs growth. In a 250 ml necked flask with vigorous shaking, 0.2 g of PVP and 0.3 mM of tri-sodium citrate were dissolved in 10 ml of deionized water. The PVP/Citrate combination was then given 100 ml of a 1 mM AgNO<sub>3</sub> solution while being vigorously stirred for 5 min. A 500 l solution of 1 mM ice-cold NaBH<sub>4</sub> was then added. The resulting colloidal solution underwent 15 minutes of stirring following the total addition of NaBH<sub>4</sub>. After being aged for around 6 months, most of the initially spherical NPs changed to triangle shapes, or prism-like structures. All of the created AgNPs were transformed into prism-



like shapes during the final 12-month extension of the ageing process.

### **Loading of Rifampicin onto silver nanoparticles**

In order to maximise the interaction between the antibiotic and the silver nanoparticles, rifampicin was added to 100 mL of synthetic AgNPs made using one of the aforementioned procedures. The mixture was continuously stirred under ultrasonication.

### **Characterization of AgNPs and Rifampicin loaded silver nanoparticles<sup>(23)</sup>**

Using a UV-Vis spectrometer double beam spectrophotometer in the 200-900 nm region, the SPR peak was detected to confirm the synthesis of AgNPs. AgNPs' morphology properties have been evaluated using TEM (JEM 2100 LB6) operating at 200 kV. Additionally, the production of rifampicin-loaded AgNPs was verified by examining how UV-VIS absorption spectrometers in the 200-900 nm range changed the photophysical characteristics of AgNPs as a result of plasmon-plasmon coupling interactions.

### **Antimicrobial activity**

The modified agar well disc diffusion method was used to conduct the antimicrobial activity test and assess the generated samples' activity. *S. aureus* (ATCC6538) and *E. coli* (ATCC 25922), which were chosen as Gram-positive bacteria and Gram-negative bacteria models, respectively, were used to study the antibacterial activity of pure AgNPs with various morphologies and composites of silver nanoparticles loaded with rifampicin. In the activity experiment, agar plates were covered with 0.5 ml solutions of the activated bacteria (1.5 10<sup>5</sup> CFU mL<sup>-1</sup>). The inoculated agar plates were gently placed on top of various filter sheets with a diameter of 5 mm that had been impregnated with 10 l of the investigated antimicrobial agents (AgNPs or rifampicin-loaded silver nanoparticles). These

composites were then incubated at 37°C. The zone of inhibition surrounding the filter paper (the width of the clear medium around the filter paper), which indicates the inhibition of bacterial growth, was used to determine the antibacterial activity of the produced samples after a 24-hour incubation. To determine the average value of the zone of inhibition, five separate antimicrobial activity tests were conducted.<sup>(24)</sup>

## **Result and Discussion**

### **Preparation of silver nanoparticles**

#### **Synthesis of silver nanoparticles using sodium-borohydride [AgNPs (Borohydride)]**

An approach involving NaBH<sub>4</sub> reduction was used to create AgNPs. NaBH<sub>4</sub> works as a reducing and capping agent to stop the particles from aggregating and expanding further. In order to stabilise the growth of AgNPs and provide a surface charge for the particles, borohydride adsorption is essential.

#### **Synthesis of silver nanoparticles using lactose [AgNPs (Lactose)]**

AgNPs can be prepared using green synthesis techniques, which have advantages over traditional techniques that use harmful chemicals. With water as an environmentally friendly solvent and lactose as a capping agent, AgNPs were created using this technique. Lactose served as a capping and reducing agent in a softly heated system since it is a disaccharide.

#### **Synthesis of silver nanoparticles using citrate-modified method [AgNPs (Citrate)]**

Trisodium citrate and NaBH<sub>4</sub> were both present in the reaction mixture; the sodium citrate primarily served as a capping substance to stop the particles from aggregating and growing further. To avoid its toxicity when used in small numbers, this approach was improved to produce more biodegradable particles with the least



quantity of NaBH<sub>4</sub>. By placing a cap of negatively charged citrate on their surfaces, AgNPs are stabilised by electrostatic contact via citrate anions that are bound to the AgNPs surface.

### Characterization of silver nanoparticles and Rifampicin loaded AgNPs

#### Morphological studies of silver nanoparticles

The produced AgNPs were analysed using TEM, which showed that spherical-like AgNPs had partially aggregated and varied in particle size from 18 to 90 nm shown in Table 1. Figure 1 (a), the excessive usage of sodium borohydride, which led to the build-up of NPs, is to blame for the high degree of particle size variation. Therefore, it is important to utilise enough borohydride. AgNPs aged during six months before remaining unchanged in size and form for a full year. A sample TEM picture of the lactose-method-prepared AgNPs is shown in Figure 1(b), and it reveals that the particles are spherical, with an average particle size of 22.5 nm, adequate

distribution, and minimal aggregation. The TEM images of AgNPs made using the citrate technique are shown in Figure 1(c). The findings showed that most particles had spherical shapes and ranged in size from 5 to 15 nm on average, whereas a small number of particles had irregular shapes and ranged in size from 50 nm and above. The majority of the NPs were transformed from spherical and irregular shapes to prism as shown in Figure 1(d), with a notable change in colour from yellow to green. TEM images of the prepared AgNPs showed that, after ageing for longer time durations, it was found that the prepared AgNPs were stable for up to 6 months. Prisms, as shown in Figure 1(e), were the most prevalent shape after a year, with the hue shifting from green to blue. Because of these findings, the novel technique should be utilised to prepare AgNPs in one of two shapes: either a sphere at the start of the reaction that is stable for six months while forming a few prisms, or a uniform prism shape after one year.

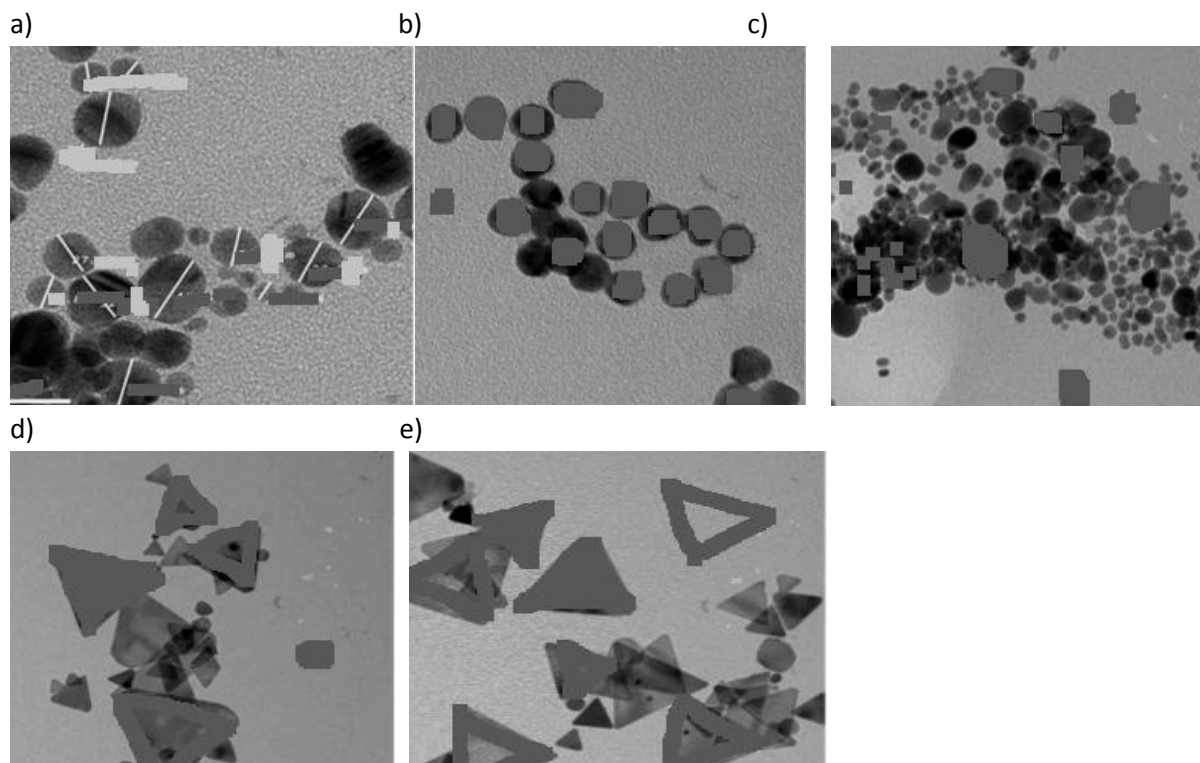


Fig.1. TEM images of (a) AgNPs (Borohydride), (b) AgNPs (Lactose) (c) AgNPs (Citrate), (d) AgNPs (Citrate) at 6 months and (e) 1 year after preparation.

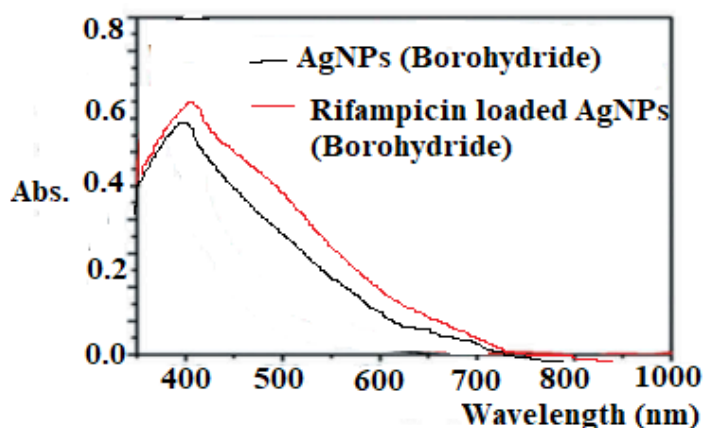


### UV – VIS spectra studies of silver nanoparticles and Rifampicin loaded AgNPs

The UV-VIS absorption spectra of rifampicin-loaded silver nanoparticles and AgNPs are shown in Figure 2. In the case of AgNPs (Borohydride), as shown in Figure 2(a), the Surface Plasmon Resonance band (SPR) of AgNPs developed in the absorption spectra of the synthesised AgNPs at around 385 nm, which is typical to the synthesis of AgNPs. After functionalizing the silver nanoparticles with rifampicin, a striking improvement in the molar absorptivity of the rifampicin-loaded silver nanoparticles (Borohydride) was observed in comparison to the bare AgNPs. This improvement was accompanied by a slight redshift from 385 nm for the bare AgNPs to 383.34 nm for the rifampicin-loaded silver nanoparticles (Borohydride). The average refractive index of the environment may have increased, the size of the NPs on the adsorption layer has grown, or the dielectric constant at the adsorption layer may have changed. Additionally, the development of a unique band at a longer wavelength of 525 nm is regarded as a crucial

characteristic that demonstrates the transformation of the hue from yellow to orange, which denotes the assembling of the particles. Figure 2(b) depicts the absorption spectrum of the AgNPs that were created using lactose as a capping agent. The SPR band that is distinctive to AgNPs appeared at 420 nm, confirming the synthesis of AgNPs. When compared to bare AgNPs, which were discovered at 375 nm, rifampicin-loaded silver nanoparticles (Lactose) showed a striking increase in molar absorptivity at max of 410.34 nm. In addition, a crucial element that shows how the colour changed from yellow to orange is the emergence of a new unique feature and broadband at a longer wavelength, or 618 nm. This band results from the connection of two nearby AgNPs' SPRs, which points to the agglomeration or assembly-related optical features of AgNPs. Figure 2(c) demonstrates a broad-bandwidth, dramatically reduced SPR intensity for rifampicin-loaded silver nanoparticles (Citrate), followed by a significant red-shift at 415 nm to a longer wavelength at 560 nm.

a)



b)



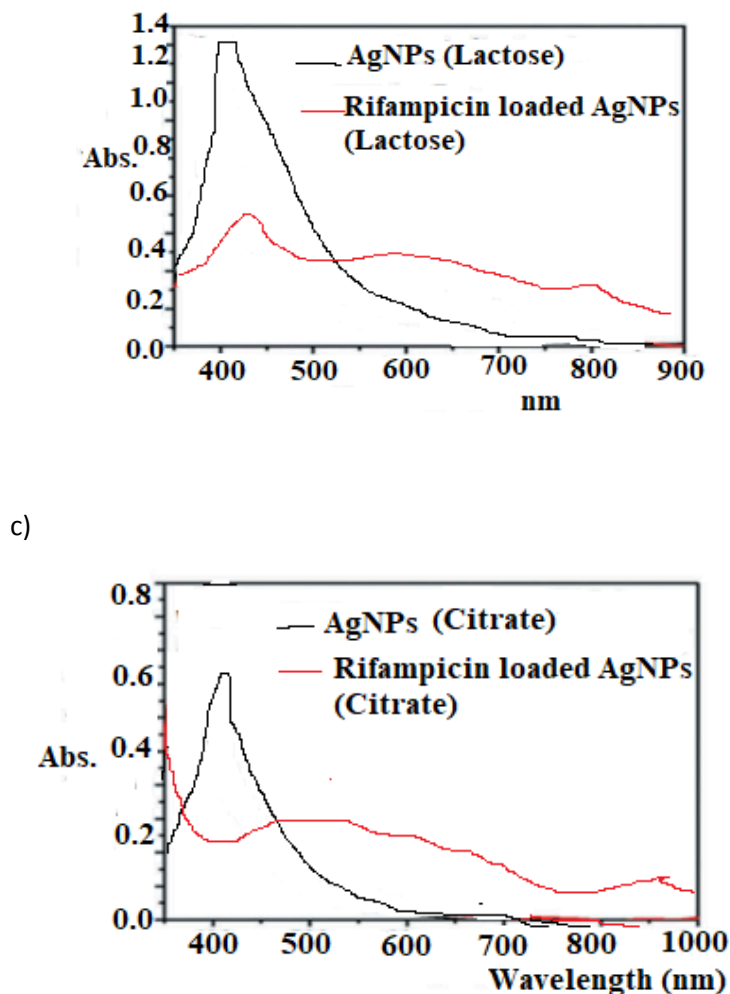


Fig. 2. The Absorption spectra of (a) AgNPs (Borohydride) & rifampicin loaded silver nanoparticles (Borohydride), (b) AgNPs (Lactose) & rifampicin loaded silver nanoparticles (Lactose), and (c) AgNPs (Citrate) & rifampicin loaded silver nanoparticles (Citrate).

### Antimicrobial assay

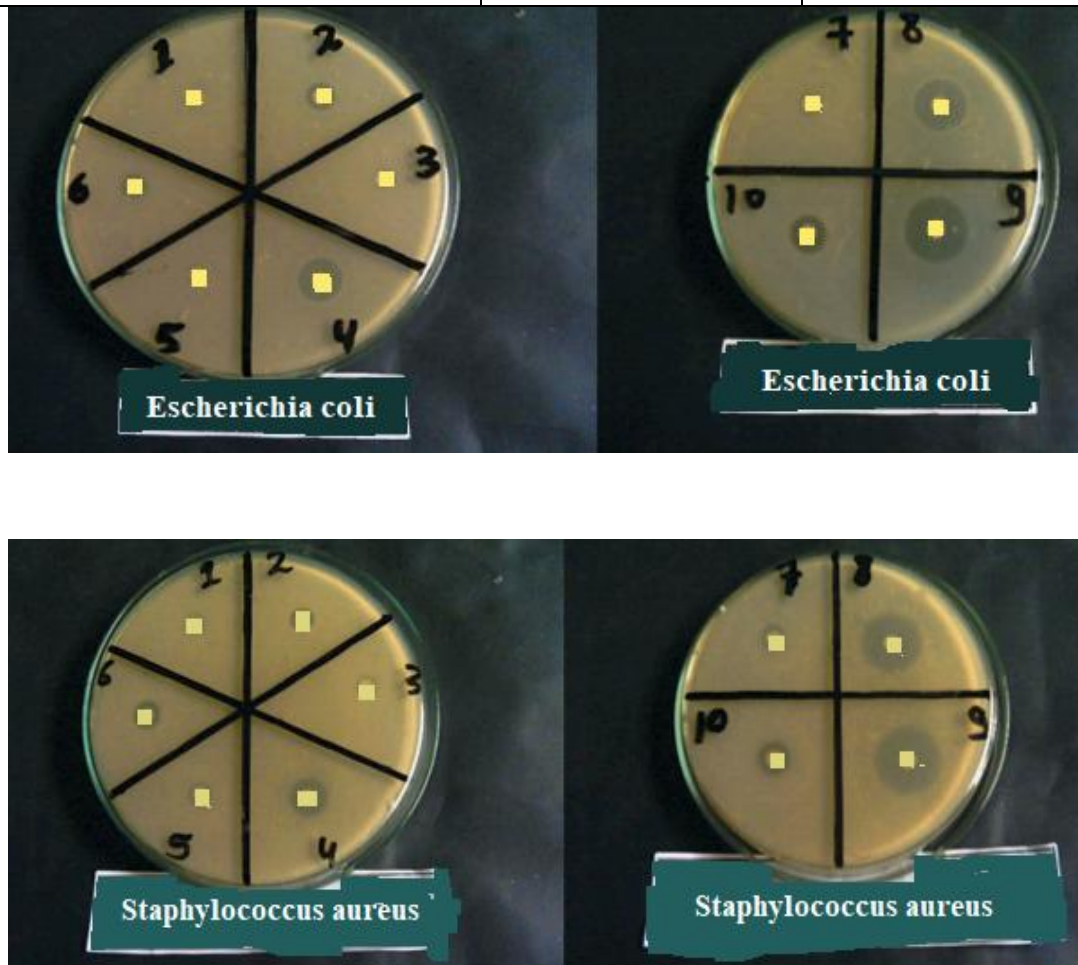
By measuring the diameter of the inhibition zone, as shown in Figures 3-4 and Table 1, the antimicrobial activity of the prepared pure AgNPs and rifampicin-loaded silver nanoparticle composites was examined in the antimicrobial activity experiment using Gram positive *S. aureus* and Gram-negative *E. coli* as models. Inhibition zones for the produced materials were evaluated during a 24-hour incubation of *E. coli* and *S. aureus* with AgNPs or rifampicin-loaded silver nanoparticles impregnated filters, as shown in Table 1 below.

Table 1. The antimicrobial activity of prepared samples in terms of zone of inhibition

Sample	<i>E. coli</i> (G-)	<i>Staph. Aureus</i> (G+)
AgNPs (Borohydride)	6	7
AgNPs (Lactose)	8	8
AgNPs (Citrate)	6	7
AgNPs (Prism)	13	12
AgNPs (Prism)	6	6
Rifampicin loaded AgNPs	9	9



(Borohydride)		
Rifampicin loaded AgNPs (Lactose)	6	7
Rifampicin loaded AgNPs (Citrate)	15	18
Rifampicin loaded AgNPs (Prism)	18	21
Rifampicin	11	10



**Fig. 3. Images of agar plates showing the antimicrobial activity of AgNPs & rifampicin loaded silver nanoparticles against Gram-positive *S. aureus* and Gram-negative *E. coli*.**

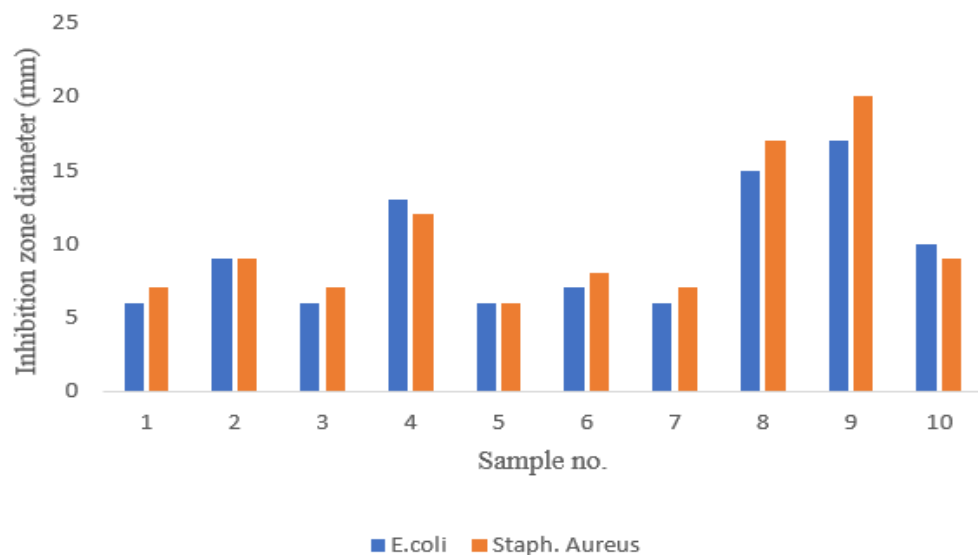
**Antimicrobial activity assessment of AgNPs**

Both types of microbes were effectively inhibited by all AgNPs samples, which is consistent with the findings of numerous other research. Figures 3-4 depict how little antimicrobial power the raw AgNPs had against both strains at the chosen concentration. Both the citrate approach and the decreased antimicrobial efficacy of the produced AgNPs caused their aggregation and big size, which prevented bacterial cell wall penetration. However, the strong antimicrobial activity of AgNPs produced by lactose led to reduced size of AgNPs and

efficient distribution of particles with a decrease in aggregation. This made it easier for AgNPs to enter the cell wall and demonstrated an increased antimicrobial activity. In addition, compared to other spherical AgNPs, prism-shaped AgNPs shown a considerable inhibitory action against Gram-negative (*E. coli*) and Gram-positive (*S. aureus*) bacteria. This may be attributed to the vertexes and edges of the nano prisms (as seen in the TEM image), which made it easier for Ag particles to enter the cell wall and damage it.







- Sample no. 1- AgNPs (Borohydride)
- Sample no. 2- AgNPs (Lactose)
- Sample no. 3- AgNPs (Citrate)
- Sample no. 4- AgNPs (Prism)
- Sample no. 5- AgNPs (Prism)
- Sample no. 6- Rifampicin loaded AgNPs (Borohydride)
- Sample no. 7- Rifampicin loaded AgNPs (Lactose)
- Sample no.8- Rifampicin loaded AgNPs (Citrate)
- Sample no. 9- Rifampicin loaded AgNPs (Prism)
- Sample no. 10- Rifampicin

**Fig. 4. The antimicrobial activity of AgNPs & Rifampicin loaded silver nanoparticle in terms of zone of inhibition.**

#### **Antimicrobial activity assessment of Rifampicin loaded silver nanoparticles**

Rifampicin modified AgNPs' synergistic antimicrobial action was investigated and evaluated against pure rifampicin. Due to the inclusion of the antibiotic rifampicin in the produced composites, rifampicin loaded silver nanoparticles (Borohydride) nanocomposite displayed a somewhat higher antimicrobial activity than pure AgNPs (Borohydride), although it is still lower than pure rifampicin. This might be accounted for by the AgNPs' own aggregation in the composite, which prevented any antibiotics from penetrating the bacterial cell wall. Unfortunately, rifampicin loaded silver nanoparticles

(Lactose) nanocomposite has lower antimicrobial activity than pure Rifampicin and AgNPs (Lactose). This might cause AgNPs (Lactose) to interact with rifampicin, which would result in less efficient AgNPs distribution and the creation of more aggregated particles than in pure AgNPs (Lactose). That denotes the assembly or agglomeration of particles that caused a decrease in the surface area of the nanocomposite, an increase in the size of the AgNPs, and ultimately a reduction in the antimicrobial activity. As opposed to pure AgNPs (Citrate) and rifampicin alone, rifampicin-loaded silver nanoparticles nanocomposite demonstrated unexpectedly



good antimicrobial effectiveness toward Gram-negative (*E. coli*) and Gram-positive (*S. aureus*) bacterial strains. As a result, the citrate was able to successfully operate as a bridge between AgNPs and rifampicin, increasing AgNPs stability via an electrostatic stabilisation mechanism brought about by the use of this anionic capping agent. On the other hand, rifampicin-loaded silver nanoparticles (Prism) nanocomposites displayed the highest antimicrobial activity compared to all other samples because Ag<sup>+</sup> was able to leach from their sharp vertexes and edges, which allowed for easier penetration of the antibiotic into the bacterial cell wall. Rifampicin-loaded silver nanoparticle composites generally shown superior antimicrobial activity than AgNPs for both Gram-negative (*E. coli*) and Gram-positive (*S. aureus*) bacterial strains, with the exception of AgNPs made by lactose technique. Rifampicin's antimicrobial activity was increased by AgNPs generated via prism-shaped citrate rather than by the antibiotic in its pure form. Additionally, rifampicin-loaded silver nanoparticle composites had higher antimicrobial efficacy against Gram-positive bacteria than Gram-negative bacteria. This is because the cell walls of the two species of bacteria differ in their molecular makeup. Although the thin Gram-negative bacteria cell wall lacks the hard and thick peptidoglycan layer found in Gram-positive bacteria, Gram-negative bacteria are distinguished by having a 10 nm thick lipopolysaccharide coating (LPS) membrane covering the peptidoglycan outer layer which makes it more difficult to be accessed by the synthesized nanocomposites.

### Conclusions

AgNPs were made using three distinct techniques before being loaded with rifampicin. The physicochemical characteristics of the produced AgNPs strongly influence their antimicrobial activity (shape, size & chemical composition). Because

of their straightforward penetration through bacterial cell walls, smaller AgNPs displayed strong antimicrobial action. The surprise high antimicrobial activity of the citrate-based, rifampicin-loaded silver nanoparticle nanocomposites against both types of microbes should be emphasised. This is a result of citrate's successful function as a link between AgNPs and rifampicin, which enhances AgNPs stability through the anionic capping agent's electrostatic stabilising mechanism. The prism-shaped citrate-based rifampicin-loaded silver nanoparticles in particular showed the most effective antimicrobial activity because of their vertexes and numerous sharp edges, which made it easier for the rifampicin-loaded silver nanoparticles to enter the bacterial cell wall and destroy it. Last but not least, it has been noted that the antimicrobial activity of a composite of silver nanoparticles loaded with rifampicin was more effective against Gram-positive bacteria than Gram-negative bacteria. This may be supported by the variations in the molecular make-up of the cell walls of the two species of bacteria.

### References

1. Kamat PV. Meeting the clean energy demand: nanostructure architectures for solar energy conversion. *J Phys Chem C*. 2007; 11:11–12.
2. Astruc D. *Nanoparticles and Catalysis*. Weinheim: John Wiley & Sons; 2008.
3. Johnson BF. *Nanoparticles in catalysis*. *Top Catal*. 2003; 24:147–159.
4. Sun C, Lee JS, Zhang M. Magnetic nanoparticles in MR imaging and drug delivery. *Adv Drug Deliv Rev*. 2008; 60:1252–1265.
5. Panyam J, Labhasetwar V. Biodegradable nanoparticles for drug and gene delivery to cells and tissue. *Adv Drug Deliv Rev*. 2003; 55:329–347.
6. Corma A, Garcia H. Supported gold nanoparticles as catalysts for organic reactions. *Chem Soc Rev*. 2008; 37:2096–2126.



7. Zhang H, Chhowalla M, Liu Z. 2D nanomaterials: graphene and transition metal dichalcogenides. *Chem Soc Rev.* 2018; 47:3015–3017.
8. H.A. Hemeg, Nanomaterials for alternative antibacterial therapy, *Int. J. Nanomedicine.* 12 (2017) 8211– 8225.
9. S. Gurunathan, Y.-J. Choi, J.-H. Kim, Antibacterial Efficacy of Silver Nanoparticles on Endometritis Caused by *Prevotella melaninogenica* and *Arcanobacterium pyogenes* in Dairy Cattle, *Int. J. Mol. Sci.* 19 (2018) 1210.
10. Hsueh PR. New Delhi metallo- $\beta$ -lactamase-1 (NDM-1): an emerging threat among Enterobacteriaceae. *J Formos Med Assoc.* 2010;109(10):685–687.
11. Poole K. Mechanisms of bacterial biocide and antibiotic resistance. *J Appl Microbiol.* 2002;92(suppl):55–64.
12. Edmundson M, Thanh NT, Song B. Nanoparticles based stem cell tracking in regenerative medicine. *Theranostics.* 2013;3(8):573–582.
13. Ramalingam B, Parandhaman T, Das SK. Antibacterial effects of biosynthesized silver nanoparticles on surface ultrastructure and nano-mechanical properties of gram-negative bacteria viz. *Escherichia coli* and *Pseudomonas aeruginosa*. *ACS Appl Mater Interfaces.* 2016;8(7):4963–4976.
14. Gurunathan S, Han JW, Dayem AA, Eppakayala V, Kim JH. Oxidative stress-mediated antibacterial activity of graphene oxide and reduced graphene oxide in *Pseudomonas aeruginosa*. *Int J Nanomedicine.* 2012;7:5901–5914.
15. Campbell EA, Korzheva N, Mustaev A, et al. Structural mechanism for rifampicin inhibition of bacterial RNA polymerase. *Cell.* 2001;104:901–912.
16. Sensi P. History of the development of rifampin. *Rev Infect Dis.* 1983;5:S402–S406.
17. Osmon DR, Berbari EF, Berendt AR, et al. Diagnosis and management of prosthetic joint infection: clinical practice guidelines by the Infectious Diseases Society of America. *Clin Infect Dis.* 2012;56:e1– e25.
18. Dunne W, Mason E, Kaplan SL. Diffusion of rifampin and vancomycin through a *Staphylococcus epidermidis* biofilm. *Antimicrob Agents Chemother.* 1993;37:2522–2526.
19. Zheng Z, Stewart PS. Penetration of rifampin through *Staphylococcus epidermidis* biofilms. *Antimicrob Agents Chemother.* 2002;46:900–903.
20. J-I S, Fujino T, Araake M, et al. Emergence of rifampicin resistance in methicillin-resistant *Staphylococcus aureus* in tuberculosis wards. *J Infect Chemother.* 2006;12:47–50.
21. Mu H, Guo F, Niu H, Liu Q, Wang S, Duan J. Chitosan improves anti-biofilm efficacy of gentamicin through facilitating antibiotic penetration. *Int J Mol Sci.* 2014;15:22296–22308.
22. Ahmed A, Khan AK, Anwar A, Ali SA, Shah MR. Biofilm inhibitory effect of chlorhexidine conjugated gold nanoparticles against *Klebsiella pneumoniae*. *Microb Pathog.* 2016;98:50–56.
23. Pharmaceutical solid polymorphism: Approach in regulatory consideration, SA Payghan, VK Kate, K Khavane, SS Purohit, *J Glob Pharm Technol* 1, 45-53
24. Nanobiocomposite: A new approach to drug delivery system, SL Patwekar, *Asian Journal of Pharmaceutics (AJP)* 10 (04)
25. Development and evaluation of nanostructured lipid carriers-based gel of isotretinoin  
SL Patwekar, SR Pedewad, S Gattani, *Particulate Science and Technology* 36 (7), 832-843
26. Review on nanoparticles used in cosmetics and dermal products, S Patwekar, S Gattani, R Giri, A  
Bade, B Sangewar, V Raut *World J. Pharm. Pharm. Sci* 3, 1407-1421
27. Solubility and Dissolution Enhancement of Poorly Water-soluble Ketoprofen by Microwave-assisted Bionanocomposites: In Vitro and In Vivo Study, SL Patwekar, *Asian Journal of Pharmaceutics (AJP)* 10 (04)

